Journal of Applied Polymer Science

Preparation and characterization of electrospun poly(ε-caprolactone)-pluronic-poly(ε-caprolactone)-based polyurethane nanofibers

Shan Xu,[1]* Jiyi Xia,[2] Sujuan Ye,[1] Ming Zhao,[1] Biqiong Wang,[1] Linglin Yang,[1] Jingbo Wu,[1] Shaozhi Fu[1]

[1]Department of Oncology, The First Affiliated Hospital of Sichuan Medical University, Sichuan Medical University, Luzhou 646000, People's Republic of China

[2]Department of Science and Technology, Sichuan Medical University, Luzhou 646000, People's Republic of China

Jiyi Xia is the co-first author for this paper. J. Xia and S. Xu contributed equally to this work.

Correspondence to: S. Z. Fu (E-mail: shaozhifu513@163.com)

ABSTRACT: In this study, amphiphilic poly(ε-caprolactone)–pluronic–poly(ε-caprolactone) (PCL–pluronic–PCL, PCFC) copolymers were synthesized by ring-opening copolymerization and then reacted with isophorone diisocyanate to form polyurethane (PU) copolymers. The molecular weight of the PU copolymers was measured by gel permeation chromatography, and the chemical structure was analyzed by ^{1}H-nuclear magnetic resonance and Fourier transform infrared spectra. Then, the PU copolymers were processed into fibrous scaffolds by the electrospinning technology. The morphology, surface wettability, mechanical strength, and cytotoxicity of the obtained PU fibrous mats were investigated by scanning electron microscopy, water contact angle analysis, tensile test, and MTT analysis. The results show that the molecular weights of PCFC and PU copolymers significantly affected the physicochemical properties of electrospun PU nanofibers. Moreover, their good *in vitro* biocompatibility showed that the as-prepared PU nanofibers have great potential for applications in tissue engineering. © 2016 Wiley Periodicals, Inc. J. Appl. Polym. Sci. **2016**, *133*, 43643.

KEYWORDS: electrospun scaffold; poly(ε-caprolactone); pluronic; polyurethane nanofibers; tissue engineering

Received 24 November 2015; accepted 11 March 2016

DOI: 10.1002/app.43643

INTRODUCTION

As a unique process technology for fibrous scaffold, electrospinning emerged in the 20th century and gained much attention because it can produce various ultrafine fibers of a large number of polymers. Electrospun fibers have diverse applications such as in drug delivery systems, tissue engineering, and high-performance batteries.[1–4] Especially, because of their high surface-to-volume ratio and high porosity and morphology similar to extracellular matrices (ECM),[5–9] electrospinning technique has been intensively studied in the field of tissue engineering.

The electrospun fibers used for tissue engineering can be massively fabricated by a variety of materials including natural polymers such as chitosan, gelatin, cellulose, and synthetic polymers like poly(lactic acid) (PLA), poly(ε-caprolactone) (PCL), and poly(D,L-lactic acid) (PDLLA).[10–14] Particularly, the synthetic polymers have been widely fabricated into fibrous scaffolds and applied in tissue engineering and drug delivery systems because of their simple preparation method, easy large-scale production, and unique mechanical property.[15–17] Among them, polyurethane (PU) is a type of block copolymer composed of rigid urethane hard segments and polyether/polyester soft segments with a low glass transition temperature.[18] PUs have been intensively studied in biomedical fields such as drug delivery and tissue engineering owing to their good hemocompatibility, cell compatibility, and unique mechanical property.[19–23] Carlberg *et al.* found that electrospun PU scaffolds exhibit have potential as the cell carriers in neural tissue engineering repair and rehabilitation of the adult human central nervous system.[24] Shah *et al.* reported that the biodegradable segmented L-tyrosine PUs (LTUs) have excellent potential for biomedical applications such as in the formulation of drug/gene delivery devices and tissue engineering scaffolds.[25] Similarly, electrospun PU membranes were used as wound dressings, with the advantages of controllable evaporative water loss, excellent oxygen permeability,

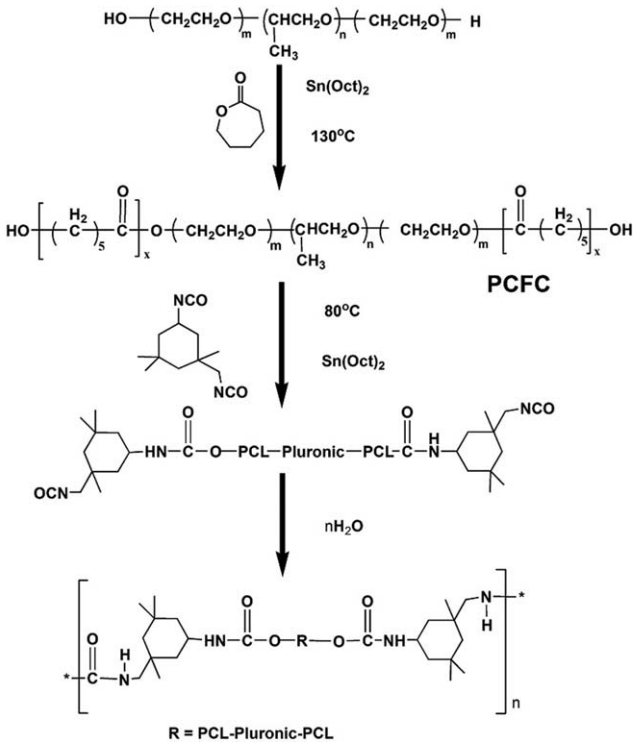

Scheme 1. Scheme of the synthesis pathway of the PCFC-based polyurethanes (PUs).

enhanced fluid drainage ability, and increased epithelialization rate; the dermis became well organized if the wounds were covered with electrospun nanofibrous membranes.[26,27]

Synthetic poly(ε-caprolactone)–pluronic–poly(ε-caprolactone) (PCL–pluronic–PCL, PCFC) copolymers have been used as the carriers for a variety of drug/gene delivery systems.[28,29] The results indicate that the polymer based on PCL and pluronic had good biodegradability and biocompatibility. However, PCFC-based PUs have not been used in the fabrication of fibrous scaffolds by electrospinning technology. In this study, the physicochemical properties and cell biocompatibility of PU fibrous membranes based on PCL–pluronic–PCL copolymers were investigated.

EXPERIMENTAL

Materials

Pluronic-105 [poly(ethylene glycol)-poly(propylene glycol)-poly (ethylene glycol), PEG-PPG-PEG, Mn = 1900], ε-caprolactone (ε-CL), isophorone diisocyanate (IPDI), and stannous octoate [$Sn(Oct)_2$] were purchased from Sigma-Aldrich. Organic solvents such as dichloromethane (CH_2Cl_2) and DMF were obtained from Kelong Chemicals (Chengdu, China). All the materials used in this article were of analytical reagent grade (AR).

Synthesis of PCFC-Based PUs

The PU copolymers were obtained in a two-step process; and the reaction scheme is shown in Scheme 1. In the first step, the prepolymers PCL–pluronic–PCL (PCFC) with different molecular weights were prepared by the ring-opening copolymerization of ε-CL initiated by pluronic-105 (PEG_{11}–PPG_{16}–PEG_{11}) following the procedure reported by Shi *et al.*[30] A typical PCL–pluronic–PCL copolymer (PCFC3K, code: P1) was prepared as follows: 5.61 g (0.0492 mol) of ε-caprolactone, 9.69 g (0.0051 mol) of pluronic-105, and 0.1 g (0.25 mmol) of $Sn(Oct)_2$ were added to a dry three-necked round-bottom flask under nitrogen atmosphere. The polymerization was performed at 130 °C under mechanical stirring. After the reaction for 5 h, the reaction system was degassed for another 1 h. After cooling the flask to room temperature under nitrogen atmosphere, the resulting PCFC copolymer was purified by the dissolution/precipitation method using CH_2Cl_2 as the solvent and precooled petroleum ether as the precipitant, followed by vacuum drying to a constant weight.

In the second process, for the synthesis of PCFC-based PUs, the obtained PCFC prepolymer was first added to a dry flask and heated to 120 °C for 30 min to ensure melting and then cooled to 80 °C under vigorous stirring. Then, IPDI was introduced into the flask with a NCO/OH ratio of 5:1 (molar ratio) under an anhydrous nitrogen flow. $Sn(Oct)_2$ (0.5% w/w of the total reactants) was also used as catalyst. After the reaction was carried out for 5 h and degassed for another 1 h, the reactant was dissolved in CH_2Cl_2 and then precipitated in cold petroleum ether. The precipitation was placed in a fuming cupboard to allow the residual solvent evaporation at room temperature. Then, the viscous product was poured into 200 mL of distilled water with vigorous stirring for 20 min, forming PU. After vacuum dried to a constant weight at room temperature, the final products were stored in airtight bags for further use.

The molecular weights of the PCFC-based PUs were determined by gel permeation chromatography (GPC, Agilent 1100 series, Agilent Technologies, Palo Alto, CA). The polymer samples were dissolved in tetrahydrofuran (THF) at a concentration of 1–2 mg/mL. The mobile phase was THF at a flow rate of 1.0 mg/mL. The column temperature was maintained at 35 °C. The molecular weights of the samples were calculated using polystyrenes as the standard with a narrow molecular weight distribution.

Electrospinning Process

The dried PCFC-based PU blocks were cut into pieces and then dissolved in a mixture of CH_2Cl_2 and DMF at a ratio of 3:1 (v/v) to ensure that the polymer was completely dissolved. The formed PU solution at a concentration of 20 mg/mL was drawn into a 20-mL plastic syringe (BD), which was mounted horizontally on an infusion pump (Smith Medical Instrument Company, Zhejiang, China). A Teflon tube was used to connect the syringe and a stainless-steel blunt-ended needle with an inner diameter of 0.5 mm. The PU solution was electrospun at a high voltage of 18 kV, driven by a high-voltage power supply (High Voltage Technology Institute, Beijing, China). The distance between the spinneret and grounded aluminum foil collector was adjusted to 12 cm. The flow rate of the PU solution was adjusted to 3–6 mL/h according to the molecular weight of the PUs. All the obtained electrospun fibers were dried in a vacuum oven at room temperature to eliminate any residual solvents and kept in a desiccator for further characterization.

Characterization of PCFC-based PU Fibrous Membranes

^{1}H-Nuclear Magnetic Resonance (^{1}H-NMR) Analysis. The ^{1}H-NMR spectrum of the PCFC-based PU copolymer was recorded

using a Varian 400 spectrometer (Varian, Palo Alto, CA) at 400 MHz using tetramethylsilane as the internal reference and $CDCl_3$ as the solvent.

Fourier Transform Infrared Spectrum (FT-IR). The FT-IR analyses of PCFC and PCFC-based PU coplymers were performed using a Nicolet 6700 FTIR spectrometer (Thermo Nicolet Corp., Madison, WI) to identify their chemical structures. The FT-IR spectra were obtained in the wavenumber range of 400–4000 cm^{-1}.

Differential Scanning Calorimetry (DSC). The thermal properties of the electrospun PU fibers with different molecular weights were characterized by using a differential scanning calorimeter (NETSCZ 204, NETSCZ, Selb, Germany). All the measurements were performed under nitrogen atmosphere at a heating rate of 10 °C/min.

Scanning Electron Microscopy (SEM). The surface morphology of the electrospun PU fibrous scaffolds was observed using a scanning electron microscope (SEM, JEM-100CX, JEOL, Tokyo, Japan). Before the observation, the samples were fixed to the SEM holder using a double-sided adhesive tape, and then the surfaces of the samples were coated with a thin layer of gold using a sputter coater (Desk II, Denton Vacuum, Moorestown, NJ). All the samples were observed at 20 kV.

Measurement of Water Contact Angle

The water contact angles of the electrospun PU membranes were measured using a water contact angle analyzer (DSA 100, Kruss, Hamburg, Germany) at room temperature. A drop of 3 μL deionized water was placed on the sample surface. The drop was photographed immediately, and the contact angle values were measured automatically. In this study, each scaffold was measured at least four times at different locations, and the results were averaged.

Mechanical Properties

The mechanical properties of the electrospun PU fibrous mats were measured using a universal mechanical testing instrument (Instron-5567, Instron, Norwood, MA) at room temperature and a relative humidity of 60%. All the specimens were cut into stripes with a length of 40 mm, a width of 5 mm, and a thickness of 0.10–0.15 mm. The mechanical properties were obtained from the stress–strain curves and averaged for five specimens.

Cell Viability Assay

To investigate the cytotoxicity of the electrospun PU fibrous mats, the fibrous scaffolds were placed at the bottom of a 24-well cell culture plate and sterilized with an ethylene oxide (ETO) steam for 24 h at room temperature; then, 1 mL of the cell suspension containing 5×10^3 of NIH 3T3 cells was seeded evenly on the samples. The blank cell culture plate was used as the control after seeding the cells. The culture medium was changed every 2 days. After seeding for 1, 3, and 5 days, 100 μL of an MTT (5 mg/mL) solution was added to each well and incubated at 37 °C for 4 h. After the removal of the supernatants, 650 μL of dimethyl sulfoxide (DMSO) was added to each well for dissolving the blue formazan crystal, and then the solution was transferred to 96-well plates. The absorbance of the contents of each well was measured at 570 nm using an ELISA microplate reader (Bio-Rad). The mean value was obtained from the measurements of four test runs.

Statistical Analysis

All the quantitative data were statistically analyzed and expressed as the mean ± standard deviation (SD). The statistical analysis was determined by single factor ANOVA. $P < 0.05$ was considered significant.

RESULTS AND DISCUSSION

Synthesis and Characterization of PCFC-Based Polyurethane Copolymers

In this study, the PCFC-based polyurethane copolymers were synthesized by a two-step reaction as shown in Scheme 1. First, the PCFC copolymers with different molecular weights were prepared by the ring-opening copolymerization of ε-CL initiated by Pluronic-105 using stannous octoate as the catalyst. Then, they were reacted with IPDI to form PCFC-based prepolymers. According to the GPC data listed in Table I, the formed polyurethanes had a high molecular weight compared to the theoretical molecular weight of original PCFC copolymers. For example, PCFC with a theoretical molecular weight of 10,000, which was determined by the feed ratio, had a final molecular weight of ~450,000 when it formed a PU copolymer, named as PU10K. Similarly, other three PCFC-based PU copolymers were named as PU3K, PU6K, and PU8K according to the theoretical molecular weights of PCFC, respectively. The ^{1}H-NMR spectrum of the PCFC-PU copolymer and the detailed assignment of characteristic absorption peaks are shown in Figure 1. The chemical shifts of the CH_3 and CH_2 protons in the PPG unit of Pluronic block were 1.15 (peak h) and 3.55 ppm (peak f), respectively. The sharp peak at 3.65 ppm (peak d) belonged to the methylene protons of —CH_2CH_2O— in the PEG unit of pluronic block. The peaks at 1.38 (peak b), 1.65 (peak b), 2.30 (peak c), and 4.05 ppm (peak e) were attributed to the methylene protons of —$(CH_2)_3$—, —$OCCH_2$—, and —CH_2OOC— in the PCL blocks, respectively.[31,32] The weak peaks at 4.20 ppm (peak a) and 3.68 ppm (peak g) were attributed to the methylene protons of —O—CH_2—CH_2— in PEG end unit linked with the PCL blocks. The peak at 1.05 ppm (peak i) belonged to the methyl protons of IPDI. Figure 2 shows the typical FT-IR spectra of PCFC and PU copolymers. In both the spectra, the absorption peaks at 1727 cm^{-1} belonged to the carbonyl (—C═O) groups of both the copolymers. A wide absorption peak between 2700 and 3050 cm^{-1} was attributed to the vibration of the carbon hydrogen (—CH_2—) in the PCL blocks. In the PCFC spectrum, the absorption peak at 3500 cm^{-1} belonged to the bending vibration of the terminal hydroxyl (—OH—) group in the PCL chains. The peak disappeared in the PU spectrum because the hydroxyl groups reacted with IPDI, and a new peak appeared at 3350 cm^{-1}, which was attributed to the stretching vibration of the N—H bonds. The appearance of these characteristic peaks confirmed the successful synthesis of PCFC-based PUs.

Morphology and Surface Wettability of Electrospun PU Nanofibers

To investigate the ability of fiber formation of PCFC-based PU copolymers with different molecular weights, the morphology

Table I. The PCFC Copolymers and their PU Copolymers in this Work

PCFC copolymers (Mn)			PCFC-based PU copolymers			
Code	Theoretical[a]	Calculated[b]	Code[c]	(total Mn)	T_m (°C)	T_c (°C)
P1	3000	2870	PU3K	175,880	--[d]	--[d]
P2	6000	4218	PU6K	183,350	48.3	8.1
P3	8000	6954	PU8K	307,290	53.3	18.7
P4	10000	9326	PU10K	450,150	54.1	20.1

[a] Theoretical molecular weight, determined by feed ratio.
[b] Calculated from H-NMR results.
[c] Actural molecular weight, determined by GPC analysis.
[d] Not determined.

of the as-prepared PU scaffolds was investigated by SEM, and the images are shown in Figure 3(A–D). Although all the PU solutions could be electrospun into fibers, their morphologies and diameters varied significantly. PU3K fibers [Figure 3(A)] had the largest diameter of ~3.03 ± 0.99 μm; moreover, severe bonding was observed between the fibers. With the increase in molecular weight, the average diameter of the PU fibers significantly decreased. PU6K, PU8K, and PU10K had nanoscale fibers with average diameters of 0.82 ± 0.36, 0.74 ± 0.19, and 0.71 ± 0.22 μm, respectively. During the spinning process, except for the molecular weight of the PU copolymers, other parameters were the same, the fiber size decreased with the increase of molecular weight of the PU copolymers. It might be owing to the optimal concentration (20 mg/mL) of spinning solution. Additionally, according to the SEM images, the fiber bonding could be observed in the PU3K membrane, with the increase of the molecular weight of the PU copolymers, the bonding phenomenon was not obvious. This indicates that the PCFC-based PU copolymer with a higher molecular weight had a higher ability of fiber formation.

The water contact angle analysis shows the surface wettability of the fibrous scaffolds. As shown in Figure 4, the contact angles of all the PU scaffolds were larger than 120°, indicating that all the scaffolds had hydrophobic surfaces. With the increase in molecular weight, the contact angle also increased. PU 8K and PU 10K had a contact angle value of ~130° revealing that molecular weight adversely affected the surface wettability of the scaffolds. The ratio of the hydrophobic chains in the PU copolymer with a lower molecular weight was less than that with a higher molecular weight. Therefore, the PU copolymer with a lower molecular weight had a lower water contact angle.

Thermal Properties of Electrospun PU Fibers

The DSC scans of all the electrospun PU scaffolds were carried out to characterize the thermal properties of the specimens. The DSC traces of all the samples are shown in Figure 5(A,B), and the data obtained from the traces are listed in Table I. During the heating process [Figure 5(A)], except for PU3K, all the other three specimens showed a clear melting peak at ~50 °C. With the increase of in molecular weight, the melting temperature (T_m) also increased from 48.3 °C (PU6K) to 54.1 °C (PU10K). The trace of PU3K did not show any melting peak, indicating that PU3K copolymer might be amorphous. Figure 5(B) shows the cooling process of the four specimens. Similar to the heating traces, PU3K did not show a clear crystallizing peak, revealing that it was noncrystalline. With the increase in

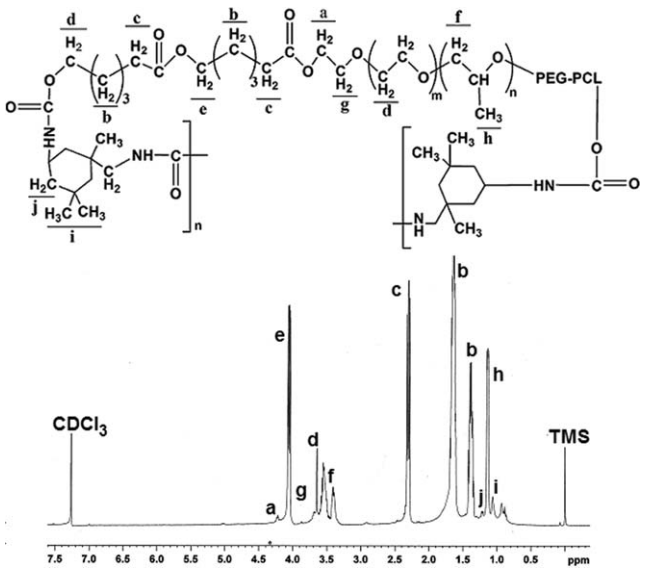

Figure 1. [1]H-NMR spectrum of the PCFC-based polyurethane copolymer.

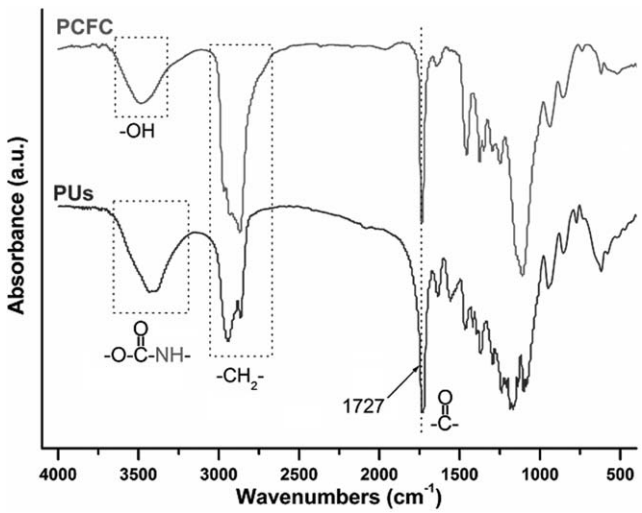

Figure 2. FT-IR spectra of the PCFC and the PCFC-based polyurethane copolymers.

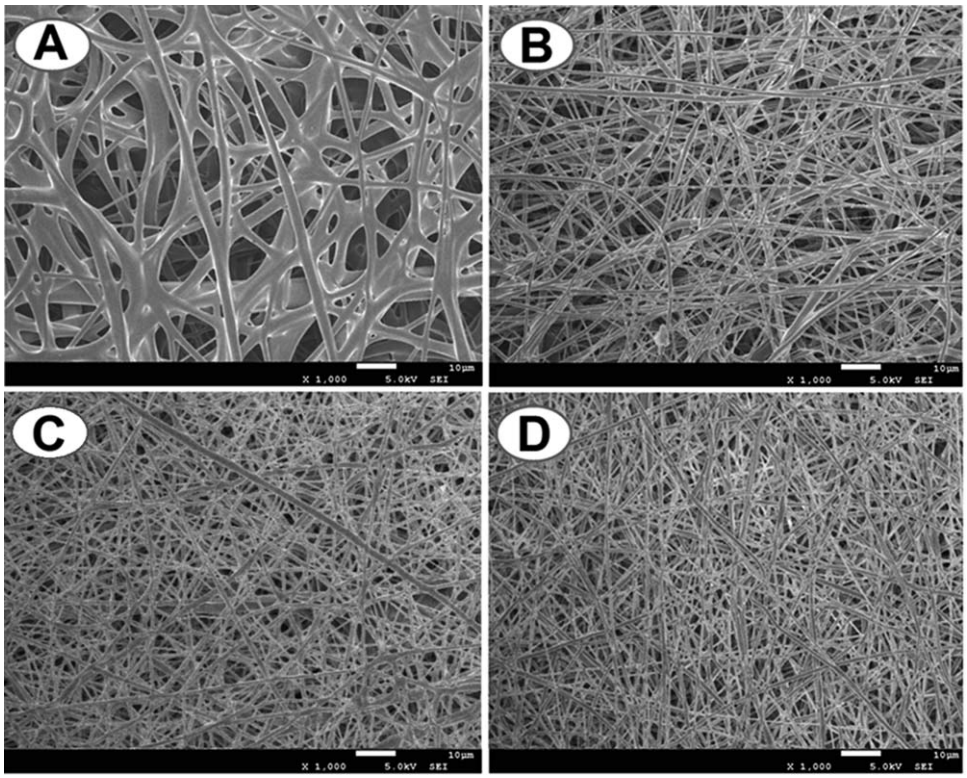

Figure 3. SEM images of the electrospun PCFC-based polyurethane fibrous scaffolds.

molecular weight, the crystallize temperature (T_c) also increased from 8.1 °C (PU6K) to 18.7 °C (PU8K), and then to 20.1 °C (PU10K), respectively. The PU copolymer with a higher molecular weight had a higher melting temperature because of the presence of longer molecular chains. The thermal motion of chains needs enough heat to release itself from the bondage of other molecular chains. Therefore, the PU copolymer with a higher molecular weight had a higher melting temperature. In the cooling process, the results indicated that the PU copolymer composed of longer PCFC chains was easier to crystallize, and the PU copolymer with a higher molecular weight had a higher crystallization temperature. It might be owing to the crystallization ability of the PCL chains, the PU copolymer composed of longer PCFC chains had a larger ratio of the PCL. On the other hands, the longer PCFC chain in the soft segment not readily mixing with the hard segment, resulting in the increase of separation between hard- and soft-segment. The separation would increase soft-segment flexibility and promote crystallization of the soft segment.[33] So, the soft segment with longer PCFC chain or a higher molecular weight had a stronger mobility. The PU copolymer with longer PCFC chains had a higher crystallization temperature.

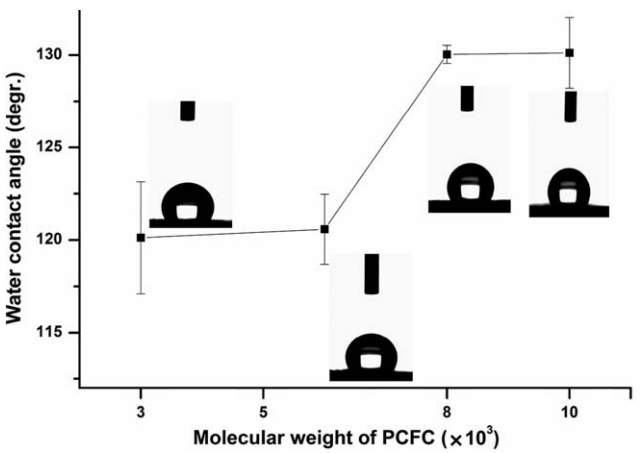

Figure 4. Water contact angles of the PCFC-based polyurethane fibrous scaffolds. Data are presented as mean ± SD, $n = 4$.

Tensile Properties of Electrospun PU Fibers

The mechanical properties of the electrospun PU scaffolds with different molecular weight were measured by tensile tests. The stress–strain curves of all the typical samples are shown in Figure 6, and the average data obtained from the curves are listed in Table II. PU3K scaffold had the smallest tensile strength at 0.82 ± 0.18 MPa and elongation rate at 117.5 ± 9.7%. Simultaneously, PU3K had the lowest Young's modulus of 0.78 ± 0.09 MPa, indicating that the scaffold was the most pliable. Along with the increase in the molecular weight of PU, both the tensile strength and elongation rate improved. PU6K scaffold had a tensile strength of 1.16 ± 0.25 MPa and an elongation of 171.7 ± 13.5%. With a further increase in molecular weight, although the tensile strength increased from 1.32 ± 0.30 MPa of PU8K to 1.63 ± 0.36 MPa of PU10K, the elongation rate suffered a loss, decreased from 165.5 ± 10.8% (PU8K) to 148.2 ± 14.6% (PU10K). The Young's modulus of the four specimens showed the same tendency as the tensile strength; the PU scaffold with the highest molecular weight had

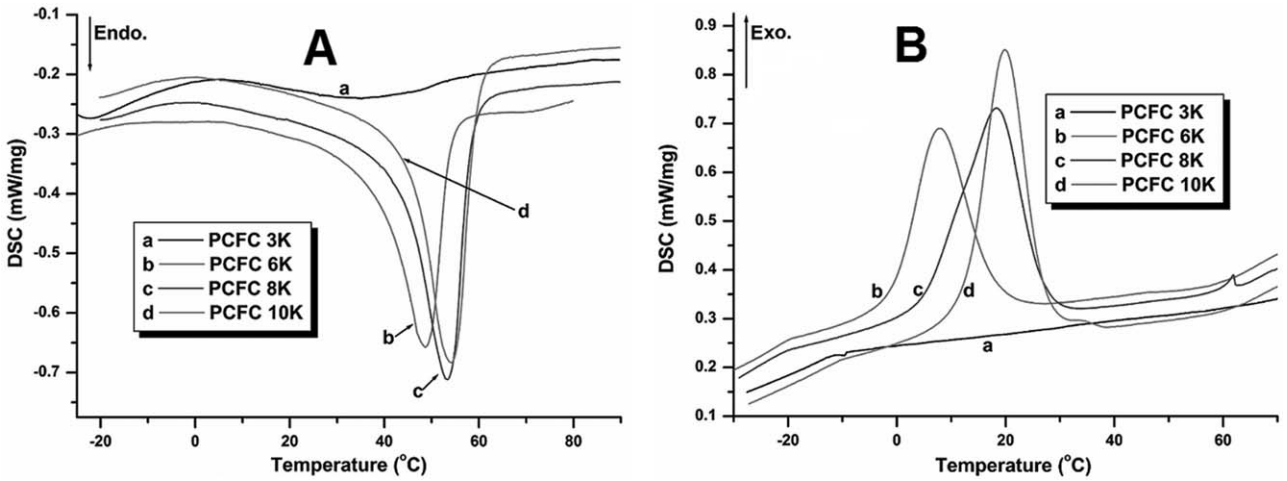

Figure 5. DSC thermograms of the PCFC-based polyurethane copolymers. (A) Heating process and (B) cooling process. The rates of heating and cooling were 10 °C/min.

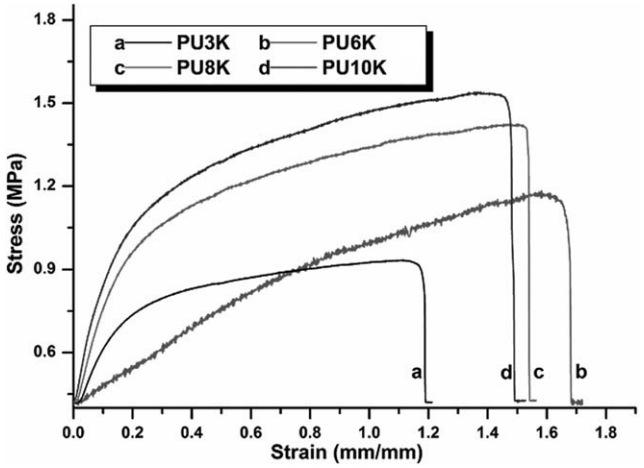

Figure 6. Strain–stress curves of the electrospun PU fibrous membranes, PU3K (a), PU6K (b), PU8K (c), and PU10K (d).

the largest Young's modulus. The results show that the molecular weight of the PU copolymer significantly affected the mechanical properties of the PU fibrous scaffolds. In addition, as evidenced by the DSC results, the PU copolymer with a higher molecular weight had a higher crystallization degree, so leading to a larger mechanical strength. In this study, the largest tensile strength and the strain at break of the PCFC-based PU nanofibers ranged from 0.9 to 1.5 MPa and 120–170%, respectively. Compared with other similar PU fibers, the elongation rate at break of the PCFC-based PU nanofibers was higher than that of the PCL-based shape memory PU fibers at a range of 85–115%.[34] However, both the tensile strength and elongation rate were much lower than those of many PU block membranes due to the electrospun membranes had an incompact porous network structure.[20,35] Just because the low tensile strength of fibrous membranes, some additives like single-walled carbon nanotube or tourmaline nanoparticles are added into PU fibers to enhance their mechanical properties in tissue engineering.[36,37]

In Vitro Cell Viability Assessment

Polymeric scaffolds for tissue engineering applications should possess good cell viability and no toxicity.[38,39] To investigate the cell cytotoxicity of the electronspun PU fibrous scaffolds, the cell viability was determined by the MTT (3-[4,-dimethylthiazol-2-yl]-2,5-diphenyltetrazolium bromide) assay. The blank wells of a cell culture plate were used as the control. Figure 7 shows the optical density (OD) value of the control and all the PU scaffolds from an MTT assay of NIH3T3 cells that were cultured for 1, 3, and 5 days. A high OD value represents a high cell viability during the cell culture on the scaffold. The cell viability of NIH 3T3 cells on all the samples showed a time-dependent pattern. On the first day, the cell viability on all the electrospun PU scaffolds was slightly lower than that of the control. At 3 days, however, the OD in all the groups clearly increased compared to those of 1 day, and PU8K had the largest cell viability. When the cells were seeded on all the samples for 5 days, the cell viability in the control group did not dramatically increase compared to that of 3 day. However, in the PU scaffolds, the cell viability increased rapidly and had an outstanding viability rate as they became approximately triple at

Table II. Mechanical Properties of Electrospun PCFC-Based PU Fibrous Membranes

PU membranes	Tensile strength (MPa)	Elongation at break (%)	Young's modulus (MPa)
PU3K	0.82 ± 0.18	117.5 ± 9.7	0.78 ± 0.09
PU6K	1.16 ± 0.25	171.7 ± 13.5	0.96 ± 0.11
PU8K	1.32 ± 0.30	165.5 ± 10.8	1.15 ± 0.08
PU10K	1.63 ± 0.36	148.2 ± 14.6	1.28 ± 0.18

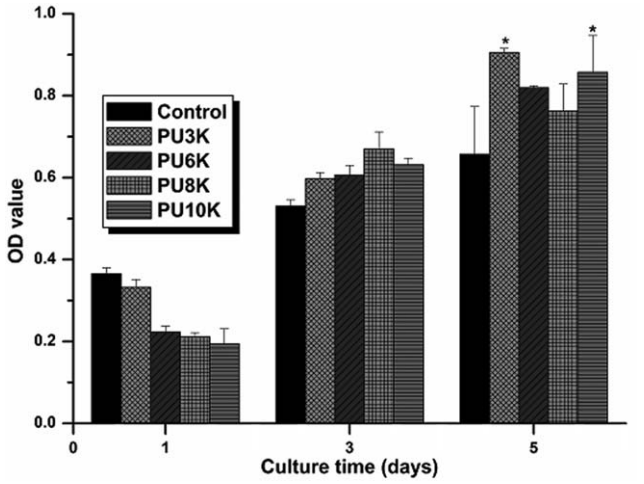

Figure 7. Comparison of NIH3T3 cell proliferation on cell culture plates (control), and PU fibrous scaffolds after cultured for 1, 3, and 5 days.

5 day. Especially, PU3K and PU10K scaffolds showed excellent cell viability compared to the other two scaffolds and control ($P < 0.05$). Compared to the control group, which was a blank cell culture plate, all the PU scaffolds showed a higher cell viability after 3 and 5 days culture. This is probably because the PU scaffolds had remarkably increased surface areas for cell attachment and significantly improved interconnected pore architecture that provides easier pathways for the diffusion of gases, transportation of nutrients and migration of cells, as a temporary and artificial ECM for growing cells. The cell viability behavior indicates that the electrospun PCFC-based PU fibrous scaffolds had good cell viability and could be promising biomaterials for tissue engineering applications.

CONCLUSIONS

In this study, amphiphilic PCFC copolymers with different molecular weights were synthesized by ring-opening copolymerization, and reacted with IPDI to form prepolymers, and then PU copolymers. The prepared PCFC-based PU copolymers were then fabricated into fibrous scaffolds using electrospinning technology. The average diameter of electrospun fibers decreased with the increase of molecular weight of the PU copolymers. All the PU fibrous membranes were hydrophobic with water contact angles larger than 120°. Except for PU3K, the other three PU copolymers had one melting peak and one crystallizing peak. The mechanical test showed that the molecular weights of PCFC and PU copolymers also significantly affected on the tensile strength and the elongation rate of the electrospun PU scaffolds. Moreover, the *in vitro* MTT assay revealed that the fibrous cells had good viability on the as-prepared PU scaffolds, and they can be used in tissue engineering.

ACKNOWLEDGMENTS

This work was financially supported by the Union Project of Luzhou City and Sichuan Medical University (14JC0144, 2013LZLY-J40), Youth Talent Fund of the First Affiliated Hospital of Sichuan Medical University (2013-60).

REFERENCES

1. Li, D.; Xia, Y. *Adv. Mater.* **2004**, *16*, 1151.
2. Huang, Z. M.; Zhang, Y. Z.; Kotaki, M.; Ramakrishna, S. *Compos. Sci. Technol.* **2003**, *63*, 2223.
3. Kim, J. S.; Reneker, D. H. *Polym. Eng. Sci.* **1999**, *39*, 849.
4. Reneker, D. H.; Chun, I. *Nanotechnology* **1996**, *7*, 216.
5. Kołbuk, D.; Sajkiewicz, P.; Maniura-Weber, K.; Fortunato, G. *Euro. Polym. J.* **2013**, *49*, 2052.
6. Sridhar, R.; Lakshminarayanan, R.; Madhaiyan, K.; Amutha Barathi, V.; Lim, K. H.; Ramakrishna, S. *Chem. Soc. Rev.* **2015**, *44*, 790.
7. Betha, S.; Reddy, B. P.; Varma, M. M.; Raju, B. D.; Kolapali, V. R. M. *J. Pharm. Invest.* **2015**, *45*, 13.
8. Naseri, N.; Mathew, A. P.; Girandon, L.; Frohlich, M.; Oksman, K. *Cellulose* **2015**, *22*, 521.
9. Chutipakdeevong, J.; Ruktanonchai, U.; Supaphol, P. *J. Appl. Polym. Sci.* **2015**, *132*, DOI: 10.1002/app.41653.
10. Li, Q.; Wang, X.; Lou, X.; Yuan, H.; Tu, H.; Li, B.; Zhang, Y. *Carbohydr. Polym.* **2015**, *130*, 166.
11. Boitard, S.; Joanne, P.; Kitsara, M.; Pernot, M.; Forest, P.; Vanneaux, V.; Larghero, J.; Menasche, P.; Chen, Y.; Agbulut, O. *Arch. Cardiovasc. Dis. Suppl.* **2015**, *7*, 198.
12. Laurila, E.; Thunberg, J.; Argent, S. P.; Champness, N. R.; Zacharias, S.; Westman, G.; Ohrstrom, L. *Adv. Eng. Mater.* **2015**, *17*, 1282.
13. Dong, Y.; Marshall, J.; Haroosh, H. J.; Mohammadzadehmoghadam, S.; Liu, D.; Qi, X.; Lau, K. T. *Compos. A: Appl. Sci.* **2015**, *76*, 28.
14. Luickx, N.; Van Den Vreken, N.; Segaert, J.; Declercq, H.; Cornelissen, M.; Verbeeck, R. *J. Biomed. Mater. Res. A:* **2015**, *103*, 2720.
15. Boakye, M. A.; Rijal, N. P.; Adhikari, U.; Bhattarai, N. *Materials* **2015**, *8*, 4080.
16. Ru, C.; Wang, F.; Pang, M.; Sun, L.; Chen, R.; Sun, Y. *ACS Appl. Mater. Interfaces* **2015**, *7*, 10872.
17. Poursorkhabi, V.; Mohanty, A. K.; Misra, M. *J. App. Polym. Sci.* **2015**, *132*, DOI: 10.1002/app.41260.
18. Sabitha, M.; Rajiv, S. *Polym. Eng. Sci.* **2015**, *55*, 541.
19. Mahanta, A. K.; Mittal, V.; Singh, N.; Dash, D.; Malik, S.; Kumar, M.; Maiti, P. *Macromolecules* **2015**, *48*, 2654.
20. Tsai, M. C.; Hung, K. C.; Hung, S. C.; Hsu, S. H. *Colloid Surf. B* **2015**, *125*, 34.
21. Jeon, H. J.; Kim, J. S.; Kim, T. G.; Kim, J. H.; Yu, W. R.; Youk, J. H. *Appl. Surf. Sci* **2008**, *254*, 5886.
22. Yao, C.; Li, X.; Neoh, K. G.; Shi, Z.; Kang, E. T. *J. Membr. Sci.* **2008**, *320*, 259.
23. Werkmeister, J. A.; Adhikari, R.; White, J. F.; Tebb, T. A.; Le, T. P. T.; Taing, H. C.; Mayadunne, R.; Gunatillake, P. A.; Danon, S. J.; Ramshaw, J. A. M. *Acta Biomater.* **2010**, *6*, 3471.
24. Carlberg, B.; Axell, M. Z.; Nannmark, U.; Liu, J.; Kuhn, H. G. *Biomed. Mater.* **2009**, *4*, 045004.
25. Shah, P. N.; Manthe, R. L.; Lopina, S. T.; Yun, Y. H. *Polymer* **2009**, *50*, 2281.

26. Unnithan, A. R.; Sasikala, A. R. K.; Murugesan, P.; Gurusany, M.; Wu, D.; Park, C. H.; Kim, C. S. *Int. J. Biol. Macromol.* **2015**, *77*, 1.
27. Kim, S. E.; Heo, D. N.; Lee, J. B.; Kim, J. R.; Park, S. H.; Jeon, S. H.; Kwon, I. K. *Biomed. Mater.* **2009**, *4*, 044106.
28. Mei, L.; Zhang, Y.; Zheng, Y.; Tian, G.; Song, C.; Yang, D.; Chen, H.; Sun, H.; Tian, Y.; Liu, K.; Li, Z.; Huang, L. *Nanoscale Res. Lett.* **2009**, *4*, 1530.
29. Zhao, J.; Gou, M. L.; Dai, M.; Li, X. Y.; Cao, M.; Huang, M. J.; Wen, Y. J.; Kan, B.; Qian, Z. Y.; Wei, Y. Q. *J. Biomed. Mater. Res. A* **2009**, *90*, 506.
30. Shi, S.; Guo, Q. F.; Kan, B.; Fu, S. Z.; Wang, X. H.; Gong, C. Y.; Deng, H. X.; Luo, F.; Zhao, X.; Wei, Y. Q.; Qian, Z. Y. *BMC Biotechnol.* **2009**, *9*, 65.
31. Liu, C. B.; Gong, C. Y.; Pan, Y. F.; Zhang, Y. D.; Wang, J. W.; Huang, M. J.; Wang, Y. S.; Wang, K.; Gou, M. L.; Tu, M. J.; Wei, Y. Q.; Qian, Z. Y. *Colloid. Surf. A* **2007**, *302*, 430.
32. Guo, Q.; Li, X.; Ding, Q.; Li, D.; Zhao, Q.; Xie, P.; Tang, X.; Luo, F.; Qian, Z. *Int. J. Biol. Macromol.* **2013**, *58*, 79.
33. Guan, J.; Wagner, W. R. *Biomacromolecules* **2005**, *6*, 2833.
34. Meng, Q.; Hu, J.; Zhu, Y.; Lu, J.; Liu, Y. *J. Appl. Polym. Sci.* **2007**, *106*, 2515.
35. Jiang, X.; Li, J.; Ding, M. M.; Tan, H.; Ling, Q.; Zhong, Y.; Fu, Q. *Eur. Polym. J.* **2007**, *43*, 1.
36. Sen, R.; Zhao, B.; Perea, D.; Itkis, M. E.; Hu, H.; Love, J.; Bekyarova, E.; Haddon, R. C. *Nano Lett.* **2004**, *4*, 459.
37. Tijing, L. D.; Ruelo, M. T. G.; Amarjargal, A.; Pant, H. R.; Park, C. H.; Dong, W. K.; Kim, C. S. *Chem. Eng. J.* **2012**, *197*, 41.
38. Li, W. J.; Laurencin, C. T.; Caterson, E. J.; Tuan, R. S.; Ko, F. K. *J. Biomed. Mater. Res.* **2002**, *60*, 613.
39. Wang, B. Y.; Fu, S. Z.; Ni, P. Y.; Peng, J. R.; Zheng, L.; Luo, F.; Liu, H.; Qian, Z. Y. *J. Biomed. Mater. Res. A* **2012**, *100*, 441.